Journal of Luminescence 130 (2010) 283–291

Contents lists available at ScienceDirect

Journal of Luminescence

journal homepage: www.elsevier.com/locate/jlumin

Optical properties of red, green and blue emitting rare earth benzenetricarboxylate compounds

Ernesto Rezende Souza [a], Ivan G.N. Silva [a], Ercules E.S. Teotonio [b], Maria C.F.C. Felinto [c], Hermi F. Brito [a,*]

[a] Departamento de Química Fundamental, Instituto de Química da Universidade de São Paulo, 05508-900, São Paulo-SP, Brazil
[b] Departamento de Química, CCEN, Universidade Federal da Paraíba, Campus João Pessoa, 58051970, João Pessoa-PB, Brazil
[c] Instituto de Pesquisas Energéticas e Nucleares, IPEN, Cidade Universitária, 05508-000 São Paulo, SP, Brazil

ARTICLE INFO

Article history:
Received 11 May 2009
Received in revised form
1 September 2009
Accepted 4 September 2009
Available online 23 September 2009

Keywords:
Rare earths
Benzenetricarboxylate
Photoluminescence
Intramolecular energy

ABSTRACT

Red, blue and green emitting rare earth compounds (RE^{3+}=Eu^{3+}, Gd^{3+} and Tb^{3+}) containing the benzenetricarboxylate ligands (BTC) [hemimellitic (EMA), trimellitic (TLA) and trimesic (TMA)] were synthesized and characterized by elemental analysis, complexometric titration, X-ray diffraction patterns, thermogravimetric analysis and infrared spectroscopy. The complexes presented the following formula: $[RE(EMA)(H_2O)_2]$, $[RE(TLA)(H_2O)_4]$ and $[RE(TMA)(H_2O)_6]$, except for Tb-TMA compound, which was obtained only as anhydrous. Phosphorescence data of Gd^{3+}-(BTC) complexes showed that the triplet states (T) of the BTC^{3-} anions have energy higher than the main emitting states of the Eu^{3+} ($^5D_0$) and Tb^{3+} ($^5D_4$), indicating that BTC ligands can act as intramolecular energy donors for these metal ions. The high values of experimental intensity parameters (Ω_2) of Eu^{3+}-(BTC) complexes indicate that the europium ion is in a highly polarizable chemical environment. Based on the luminescence spectra, the energy transfer from the T state of BTC ligands to the excited $^5D_0$ and $^5D_4$ levels of the Eu^{3+} and Tb^{3+} ions is discussed. The emission quantum efficiencies (η) of the $^5D_0$ emitting level of the Eu^{3+} ion have been also determined. In the case of the Tb^{3+} ion, the photoluminescence data show the high emission intensity of the characteristic transitions $^5D_4 \rightarrow {}^7F_J$ (J=0–6), indicating that the BTC ligands are good sensitizers. The RE^{3+}-(BTC) complexes act as efficient light conversion molecular devices (LCMDs) and can be used as tricolor luminescent materials.

© 2009 Elsevier B.V. All rights reserved.

1. Introduction

Recently, metal carboxylate compounds have been widely recognized as one of the most promising and rapidly emerging research areas in the field of coordination chemistry. The great interest for these complexes is mainly owing to excellent properties, such as high luminescence intensity and porosity, contributing to an increase in the chemical and physical versatilities as compared to classical solid materials. The carboxylate complexes have already encountered several applications such as gas storage [1–3], molecular separation, catalyses [4], photoluminescence spectroscopy, magnetism, nonlinear optics, biomarkers, etc. An important feature of materials based on carboxylate ligands is the great facility in the synthesis of so-called metal-organic framework (MOF) materials [5,6]. The attractive structural properties of MOFs provide several industrial applications to these materials, which have been generally attributed to zeolite-related inorganic solids. However, as compared to zeolites, MOFs can present a huge kind of metal ions in their composition.

Although there is a great diversity of organic ligands that can be used as functionalized organic linkers, the particular attention given to carboxylate ligands is due to their coordination ability with transition metal and trivalent rare earth ions, coordinating to the metal centers by more than one bonding modes, such as unidentate, chelating, bridging or chelating/bridging bidentate. However, extensive efforts have been dedicated toward preparation of materials presenting three-dimensional structures using polycarboxylate ligands, especially tricarboxylate anion. Recent works [7–15] have been mainly focused on metal-organic compounds with 1,2,3-benzenetricarboxylic acid (hemimellitic acid), 1,2,4-benzenetricarboxylic acid (trimellitic acid) and 1,3,5-benzenetricarboxylic (trimesic acid) (Fig. 1). The majority of these works report the syntheses, structure and thermal properties of these systems.

Among the metal centers, trivalent rare earth ions (RE^{3+}) are largely explored owing to the structural and photoluminescence properties. The research on RE-carboxylate compounds has improved dramatically, and in this field, RE^{3+} ions generally act as network nodes bridged by spacer ligands. It is important to mention that the unusual structural features frequently obtained for RE-carboxylate are due to the combination of both high coordination numbers (from 8 to 10) of the RE^{3+} ions with low

* Corresponding author. Tel.: +55 11 3091 3708; fax: +55 11 3815 5579.
E-mail address: hefbrito@iq.usp.br (H.F. Brito).

0022-2313/$ - see front matter © 2009 Elsevier B.V. All rights reserved.
doi:10.1016/j.jlumin.2009.09.004

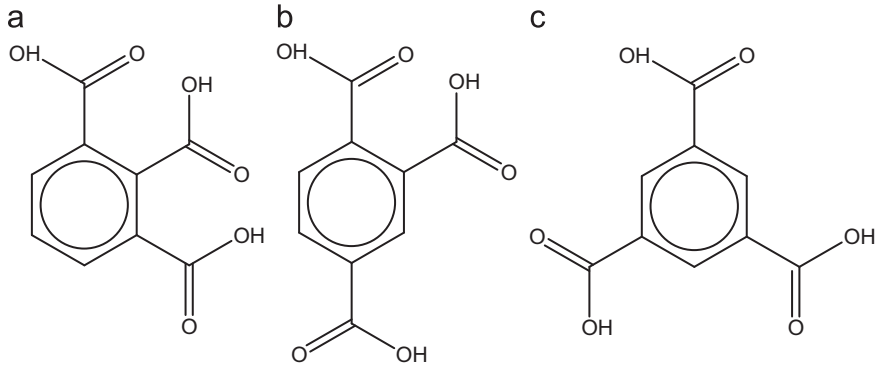

Fig. 1. Structural formulas of the tricarboxylate ligands: (a) 1,2,3-benzenetricarboxylate (EMA); (b) 1,2,4-benzenetricarboxylate (TLA) and (c) 1,3,5-benzenetricarboxylate (TMA).

stereochemical preference and the various coordination modes of the ligands [16].

A great number of luminescent RE^{3+}-complexes investigated in the literature [17–21] present Eu^{3+} and Tb^{3+} ions as emitting center owing to the very intense red and green colors displayed by their compounds, respectively. Besides, the main emitting level ($^5D_0$) of the Eu^{3+} ion is non-degenerate, which means that the emission bands assigned to the transitions $^5D_0 \rightarrow {}^7F_J$ ($0 \leq J \leq 4$) can provide information about the local symmetry by the split of the emission bands. Furthermore, a long lifetime of the emitting level, around milliseconds, is observed. Consequently, these coordination compounds play a crucial role in different fields, such as, biomedical analysis, organic light-emitting diodes (OLEDs) and sensors [22,23].

In contrast to the Eu^{3+} ion, detailed analyses of the energy-level structure and site of symmetry around the Tb^{3+} ion are complicated since the $^5D_4$ emitting level is nine-fold degenerate. In addition, this excited level is higher in energy than the $^5D_0$ emitting level of the Eu^{3+} ion. Thus, a donor energy ligand that can act as *antenna* for both Eu^{3+} and Tb^{3+} ions is expected to have its excited triplet state (T) with energy around 21,000 cm^{-1}. Some aromatic carboxylate ligands have shown donor T state with high energy, and these ligands can act as potential luminescence sensitizers for both Eu^{3+} and Tb^{3+} ions that exhibit red and green emission colors, respectively. Recently, RE^{3+}-(1,3,5-tricarboxylate) compounds have been prepared by hydrothermal method in which a mixture of rare earth salt and H_3BTC ligand is heated in a sealed vial. The sieving and sensor function to small molecules and anions were investigated based on the luminescence intensity [6,24].

In this paper, we report the synthesis, characterization and photoluminescence properties of rare earth complexes with three different tricarboxylate ligands (EMA, TLA and TMA). Red, blue and green emission colors at room temperature are observed for the Eu^{3+}, Gd^{3+} and Tb^{3+} ions, respectively. Furthermore, for Eu^{3+} ion, the experimental intensity parameters (Ω_λ), quantum emission efficiency (η), lifetimes of emitting $^5D_0$ levels, radiative (A_{rad}) and non-radiative (A_{nrad}) coefficients have also been reported. The CIE color coordinates (x, y) were determined from the emission spectra.

2. Experimental section

2.1. Preparation

The following commercially available chemicals were used without further purification. 1,2,3-benzenetricarboxylic acid (H_3EMA) was purchased from Fluka while 1,3,5-benzenotricarboxylic (H_3TMA) acid and 1,2,4-benzenotricarboxylic anhydride, precursor of 1,2,4-benzenotricarboxylic acid (H_3TLA) were purchased from Alfa Aesar. Solid [$RECl_3 \cdot (H_2O)_6$] compounds were synthesized as described in the literature [25].

2.1.1. Preparation of RE(EMA) complexes

1.5 g (~7.5 mmol) of 1,2,3-benzenetricarboxylic acid (hememelitic acid, H_3EMA) was dissolved in 200 mL of distilled water. To deprotonate the acid, NaOH 0.1 mol L^{-1} was added dropwise until pH ~6.0. To this mixture was added dropwise 50 mL of an equimolar aqueous solution of rare earth chloride (~7.5 mmol), under stirring. A few minutes after the beginning of the process, a starting white precipitate was observed. In order to increase the yield, the resulting reaction mixture was refluxed for 2 h. The solid product was filtered, washed with hot water several times and dried under vacuum for 12 h. All RE(EMA) complexes were stable in air, non-hygroscopic and insoluble in common organic solvents such as acetone, DMSO, acetonitrile, chloroform and ethanol.

[$Eu(EMA)(H_2O)_2$] Elemental analysis calcd for $C_9H_7O_8Eu$: C, 27.36%; H, 1.79%; Eu, 38.46%. Found: C, 27.44%; H, 2.07%; Eu, 37.93%. IR (KBr, cm^{-1}): 3634m, 3433b, 1533s, 1583m, 1489s, 1459m,1363s, 1068w, 768m, 716m.

[$Gd(EMA)(H_2O)_2$] Elemental analysis calcd for $C_9H_7O_8Gd$: C, 27.00%; H, 1.76%; Gd, 39.27%. Found: C, 26.82%; H, 2.00%; Gd, 38.97%. IR (KBr, cm^{-1}): 3634m, 3434b, 1583m, 1533s, 1491s, 1462m, 1364s, 1068w, 768m, 715m.

[$Tb(EMA)(H_2O)_2$] Elemental analysis calcd for $C_9H_7O_8Tb$: C, 26.88%; H, 1.75%; Tb, 39.53%. Found: C, 26.93%; H, 2.12%; Tb, 39.19%. IR (KBr, cm^{-1}): 3431b, 1582m, 1537s, 1491s, 1459m, 1364s, 1068w, 766m, 717m, 3634m.

2.1.2. Preparation of the RE(TLA) complexes

1,2,4-benzenotricarboxylic acid (trimelitic acid, H_3TLA) was obtained by the dissolution of 1.4 g (~7.5 mmol) of 1,2,4-benzenetricarboxylic anhydride in 200 mL of distilled water, and the pH was adjusted to 6.0 by adding dropwise NaOH 0.1 mol L^{-1}. To this mixture was added dropwise 50 mL of an aqueous solution of rare earth chloride (0.15 mol/L) under stirring. The white precipitate forms after addition of approximately 10 mL of the rare earth solution. The resulting reaction mixture was refluxed for 2 h, and then the solid product was filtered, washed with hot water several times and dried under vacuum. All complexes were stable in air, non-hygroscopic and insoluble in common organic solvents such as acetone, DMSO, acetonitrile, chloroform and ethanol.

[$Eu(TLA)(H_2O)_4$] Elemental analysis calcd for $C_9H_{11}O_{10}Eu$: C, 25.07%; H, 2.57%; Eu, 35.25%. Found: C, 25.37%; H, 2.75%; Eu, 35.29%. IR (KBr, cm^{-1}): 3448b, 3101w, 1586s, 1529s, 1496s, 1416s, 1079w, 844m, 789m.

[Gd(TLA)$(H_2O)_4$] Elemental analysis calcd for $C_9H_{11}O_{10}Gd$: C, 24.77%; H, 2.54%; Gd, 36.03%. Found: C, 24.79%; H, 2.57%; Gd, 36.24%. IR (KBr, cm^{-1}): 3446b, 3098w, 1586s, 1528s, 1496s, 1417s, 1079w, 845m, 790m.

[Tb(TLA)$(H_2O)_4$] Elemental analysis calcd for $C_9H_{11}O_{10}Tb$: C, 24.67%; H, 2.53%; Tb, 36.28%. Found: C, 24.60%; H, 2.49%; Tb, 36.69%. IR (KBr, cm^{-1}): 3443b, 3099w, 1586s, 1531s, 1496s, 1417s, 1079w, 846m, 790m.

2.1.3. Preparation of RE(TMA) complexes

1.5 g (~7.5 mmol) of 1,3,5-benzenetricarboxylic acid (trimesic acid, H_3TMA) was dissolved in 250 mL of distilled water and the pH was adjusted to 6.0 by adding dropwise NaOH 0.1 mol L^{-1}. To this mixture was added dropwise 50 mL of an aqueous solution of rare earth chloride under stirring. In this case, the white precipitate forms immediately with the addition of the rare earth solution. The resulting reaction mixture was refluxed for 2 h, and then the solid product was filtered, washed with hot water several times and dried under vacuum. All complexes were stable in air, non-hygroscopic and insoluble in common organic solvents such as acetone, DMSO, acetonitrile, chloroform and ethanol.

[Eu(TMA)$(H_2O)_6$] Elemental analysis calcd for $C_9H_{15}O_{12}Eu$: C, 23.14%; H, 3.24%; Eu, 32.53%. Found: C, 23.24%; H, 3.23%; Eu, 32.75%. IR (KBr, cm^{-1}): 3410b, 3263w, 3132w, 2926w, 1614s, 1561s, 1435s, 1375s, 1110w, 762m, 709m.

[Gd(TMA)$(H_2O)_6$] Elemental analysis calcd for $C_9H_{15}O_{12}Gd$: C, 22.88%; H, 3.20%; Gd, 33.28%. Found: C, 23.08%; H, 3.24%; Gd, 33.60%. IR (KBr, cm^{-1}): 3409b, 3265w, 3133w, 2925w, 1614s, 1562s, 1437s, 1376s, 1110s, 762m, 709m.

[Tb(TMA)] Elemental analysis calcd for $C_9H_3O_6Tb$: C, 29.53%; H, 0.83%; Tb, 43.42%. Found: C, 29.30%; H, 0.95%; Tb, 42.86%. IR (KBr, cm^{-1}): 1618s, 1549s, 1453s, 1389s, 1127m, 763s, 737s, 710s.

2.2. Characterization

Thermal analysis was performed on a thermobalance Schimadzu TGA-50. The samples were placed in platinum containers, and the TG curves were recorded in a dynamic synthetic air atmosphere of 50 cm^3 min^{-1} under a heating rate of 10 °C min^{-1} in the temperature range from 25 up to 900 °C. Elemental analysis was carried out using a Perkin Elmer 240 microanalyzer. Infrared spectra were recorded in KBr pellets on a Bomen model MB-102 spectrophotometer in the range from 4000 up to 350 cm^{-1}. XRD patterns of the powders were recorded on a Rigaku Miniflex diffractometer using Cu Kα radiation (30 kV and 15 mA) from 2° to 90° (2 h) and 1 s of pass time. Steady-state excitation and emission spectra of the complexes in solid state at room (298 K) and liquid nitrogen temperatures were recorded at an angle of 22.5° (front face) with a spectrofluorimeter (SPEX-Fluorolog 2) with double grating 0.22 m monochromator (SPEX 1680), and a 450 W Xenon lamp as excitation source. All spectra were recorded using a detector mode correction. The luminescence decay curves of the emitting levels were measured using a phosphorimeter SPEX 1934D accessory coupled to the spectrofluorometer.

3. Results and discussion

3.1. Characterization of RE^{3+}-BTC complexes

The elemental analyses of CHN, after mineralization of the compounds and the complexometric titration with disodium ethylenediaminetetraacetic acid (EDTA) salt, confirm the general formulas [RE(BTC)$(H_2O)_n$] for the complexes (where BTC=TMA, TLA and EMA; n=2, 4 and 6), except for the [Tb(TMA)] anhydrous complex.

XRD patterns of the [RE(BTC)$(H_2O)_n$] complexes in powder form present three isomorphic series when containing the same ligand and similar number of water molecules, except for the anhydrous [Tb(TMA)] complex (figure not shown).

The thermogravimetric curves of the [RE(BTC)$(H_2O)_n$] complexes were recorded in the temperature interval from 25 to 900 °C. As shown in Fig. 2a, the [Eu(EMA)$(H_2O)_2$] compound exhibits two mass loss events assigned to the loss of two water molecules at 245 °C and to the EMA ligand decomposition at 416 °C, producing europium oxide around 650 °C. This reveals that there are two water molecules coordinated to the Eu^{3+} ion, which corroborates with elemental analysis. In the [Eu(TLA)$(H_2O)_4$] complex (Fig. 2b), three thermal events for dehydration at 72, 148 and 250 °C correspond to the loss of one, two and one water molecules, respectively, were observed. In addition, there is another event at 508 °C assigned to TLA ligand decomposition. The same thermal behavior is observed for the gadolinium and terbium complexes. In the case of [Eu(TMA)$(H_2O)_6$] compound (Fig. 2c) there were only two dehydration events where four are lost at 112 °C and the remaining two water molecules at 131 °C. In this complex, TMA ligand decomposition occurs at 464 °C. The same thermal behavior is observed for the gadolinium and terbium coordination compounds, except for the [Tb(TMA)] complex, which presents no dehydration event, but only one at 464 °C assigned to the TMA ligand decomposition, indicating that this compound is anhydrous (Fig. 2d).

Infrared spectra of [RE(BTC)$(H_2O)_n$] complexes exhibit a broad band in the spectral range from 3500 to 3300 cm^{-1} due the O–H stretching vibration of water molecule, indicating that these complexes are hydrated. Furthermore, IR data of the [RE(EMA)$(H_2O)_2$] display a sharp band around 3634 cm^{-1}, which is assigned to free O–H stretching vibration of H_2O molecule coordinated to the rare earth ions, indicating that the water molecules do not take part in hydrogen bonding. On the other hand, the absence of the broad band in the region 3000–3500 cm^{-1} for the [Tb(TMA)] complexes indicates that this complex is anhydrous [26].

The coordination of the ligand to the rare earth ion was investigated comparing the infrared spectra of the complexes with those of the sodium-BTC salts as suggested by Deacon and Phillips [27]. The IR spectra of the BTC ligands in ionic form present strong bands at 1568 and 1382 cm^{-1} for EMA, 1583 and 1392 cm^{-1} for TLA and 1568 and 1373 cm^{-1} for TMA, which are attributed to the ν_s(C=O) and ν_{as}(C=O) vibrational modes, respectively. For the RE^{3+}-EMA complexes, $\Delta\nu$ values of around 170 and 126 cm^{-1} are observed, suggesting that the carboxylate groups are coordinated to metal ions as bidentate bridge and chelate forms through oxygen atoms. On the other hand, the RE^{3+}-TLA complexes exhibit values of $\Delta\nu$ around 112 cm^{-1}, which are significantly lesser than ionic values ($\Delta\nu$=190 cm^{-1}), suggesting coordination in chelating form. In the case of [RE(TMA)$(H_2O)_6$] (RE^{3+}=Eu and Gd) the TMA ligand presents the bidentate bridge coordination form ($\Delta\nu$=186 cm^{-1}), and the anhydrous [Tb(TMA)] complex presents chelating.

The [Tb(TMA)] complex is anhydrous mainly because of the diminution of the ionic radius of the Tb^{3+} ion, which increases the steric repulsion when compared with those of Eu^{3+} and Gd^{3+} hexahydrated complexes. Therefore, the general formula [RE(TMA)] can also be expected for other heavy rare earth ions where RE^{3+}=Dy–Lu. Therefore, the spatial conformation of the coordination TMA ligands change in a way that the water molecules are excluded from the first coordination shell of the complex structure of [Tb(TMA)]. The anhydrous behavior of these complexes is also supported by IR data.

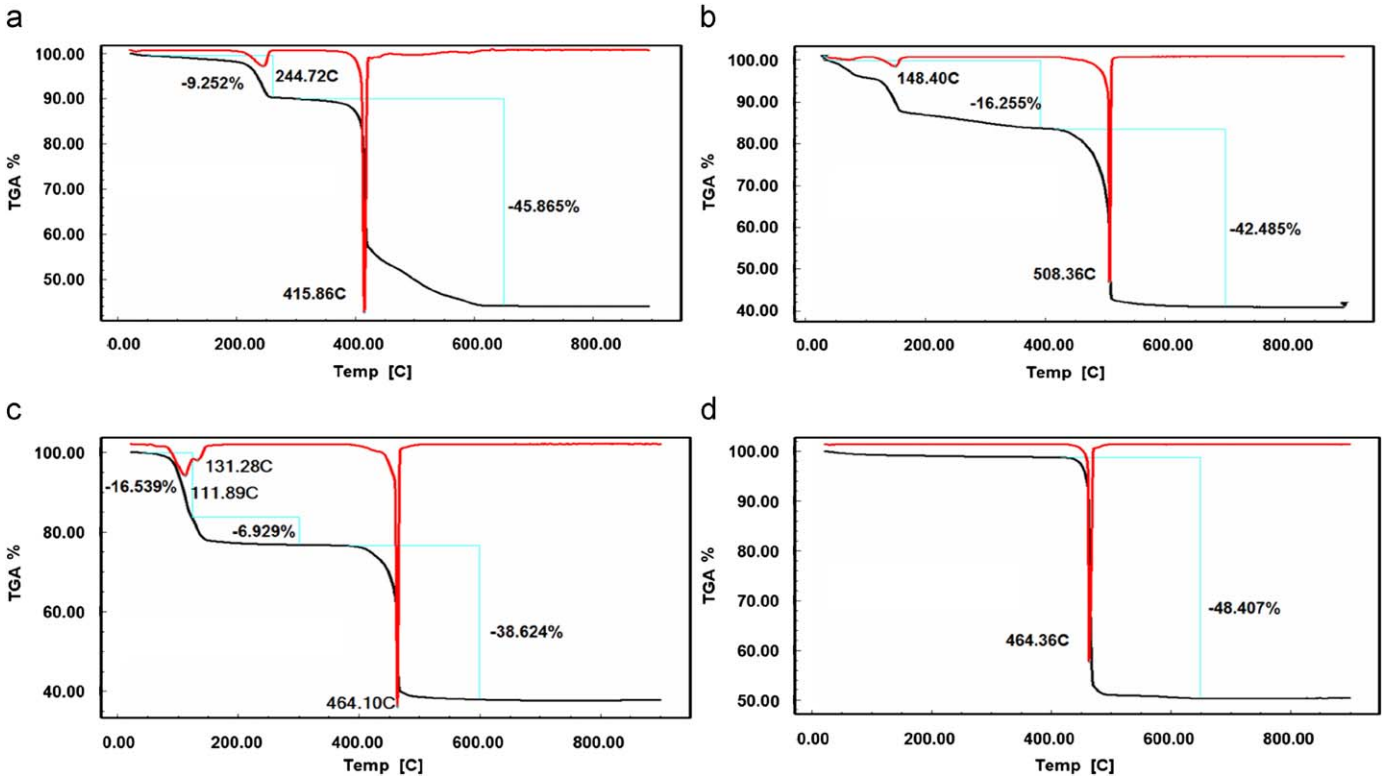

Fig. 2. Thermogravimetric curves of the [Eu(BTC)$(H_2O)_n$] complexes (n=2, 4 and 6) in solid state. All these curves were recorded at synthetic air dynamic atmosphere in the temperature interval from 20 to 900 °C.

3.2. Photoluminescence investigation

3.2.1. Phosphorescence of the Gadolinium complexes

The goal in the investigation of the photoluminescence of the Gd-BTC coordination compounds is to determine the energy of the excited states that belong to the BTC ligands. It is important to mention that the Gd^{3+} ion generally does not accept energy from organic ligands because the energy of the T states of these donor species is below the first excited $^6P_{7/2}$ state of the Gd^{3+} ion. Since there is a large energy gap ($\sim$32,000 cm^{-1}) between the $^8S_{7/2}$ ground state and the first $^6P_{7/2}$ excited state of the Gd^{3+} ion [25,28,29], it cannot be widened by energy from the lower lying first excited T_1 state of the BTC ligands via intramolecular ligand-to-metal energy transfer.

Gd-BTC emission spectra exhibit only broad bands owing to the ligand centered transitions, giving information about triplet ligand donor state positions as compared with acceptor excited rare earth states. Fig. 3a–c shows the steady-state phosphorescence spectra of Gd^{3+} BTC-complexes recorded at liquid nitrogen temperature at 350–700 nm under excitation at around 290 nm. These spectra display two overlapped broad bands with maxima around 410 and 475 nm that are assigned to the vibronic contribution and phosphorescence due to the $T \rightarrow S_0$ (π,π^*) centered ligand transitions, respectively. This behavior has been observed for other rare earth carboxylate complexes reported in the literature [30]. The luminescence decay curves of the Gd-BTC compounds recorded with emission monitored at 475 nm showed long values of the emitting state lifetime at room temperature, 298 K (Table 1): for [Gd(EMA)$(H_2O)_2$] (τ=7.113 ms), [Gd(TLA)$(H_2O)_4$] (τ=2.210 ms) and [Gd(TMA)$(H_2O)_6$] (τ=4.062 ms) and increase when recorded at low temperature (77 K) τ=8.351, 12.025 and 7.386 ms, respectively. These data confirm the triplet character of the emitting states that contribute to those bands around 475 nm.

In order to determine unequivocally the energy due to the triplet 0–0 phonon transition for each Gd^{3+}-BTC compound, time-resolved spectra (Fig. 3d–f) were recorded at liquid nitrogen temperature with excitation and emission monitored at 290 and 475 nm, respectively, using a delay of 1.0 ms. In this case, fluorescence bands decrease very fast as the flash delay is increased and only the phosphorescence from BTC ligands is displayed. The T states energy estimated from the shortest wavelength on the base of the emission bands 0–0 phonon transition is as follows: 25,694 cm^{-1} [Gd(EMA)$(H_2O)_2$]; 25,523 cm^{-1} [Gd(TLA)$(H_2O)_4$] and 25,100 cm^{-1} [Gd(TMA)$(H_2O)_6$]. As can be observed, these triplet states have energy higher than the main emitting states of the Eu^{3+} ($^5D_0$) and Tb^{3+} ($^5D_4$), indicating that BTC ligands can act as intramolecular energy donors for these rare earth metal ions.

3.2.2. Luminescence of Eu^{3+}-BTC complexes

Excitation spectra of the [Eu(BTC)$(H_2O)_n$] complexes (n=2, 4 and 6) in solid state were recorded at 77 K in the spectral range 240–600 nm under emission on the hypersensitive $^5D_0 \rightarrow {}^7F_2$ transition of the Eu^{3+} ion, at $\sim$617 nm (Figs. 4a, b and c). These spectra present a strong broad band between 270 and 400 nm assigned to the photoexcitation process of the Eu^{3+} ion via the $S_0 \rightarrow S_1$ transition. Narrow bands can also be seen assigned to the following intraconfigurational transitions (in nm): $^7F_0 \rightarrow {}^5D_0$ (578), $^7F_0 \rightarrow {}^5D_1$ (525), $^7F_0 \rightarrow {}^5D_2$ (464), $^7F_0 \rightarrow {}^5D_3$ (409), $^7F_0 \rightarrow {}^5L_6$ (494), $^7F_0 \rightarrow {}^5L_7$ (373), $^7F_0 \rightarrow {}^5D_4$ (360), $^7F_0 \rightarrow {}^5H_3$ (317) and $^7F_0 \rightarrow {}^5F_2$ (295). However, these bands are less intense than those bands corresponding to the $S_0 \rightarrow S_1$ transition. The excitation spectra of TMA and TLA complexes display higher luminescence intensity around 300 nm than from 4f–4f transitions; however, the broad band of EMA shows lower intensity than that of europium electronic transitions. This result gives evidence that europium

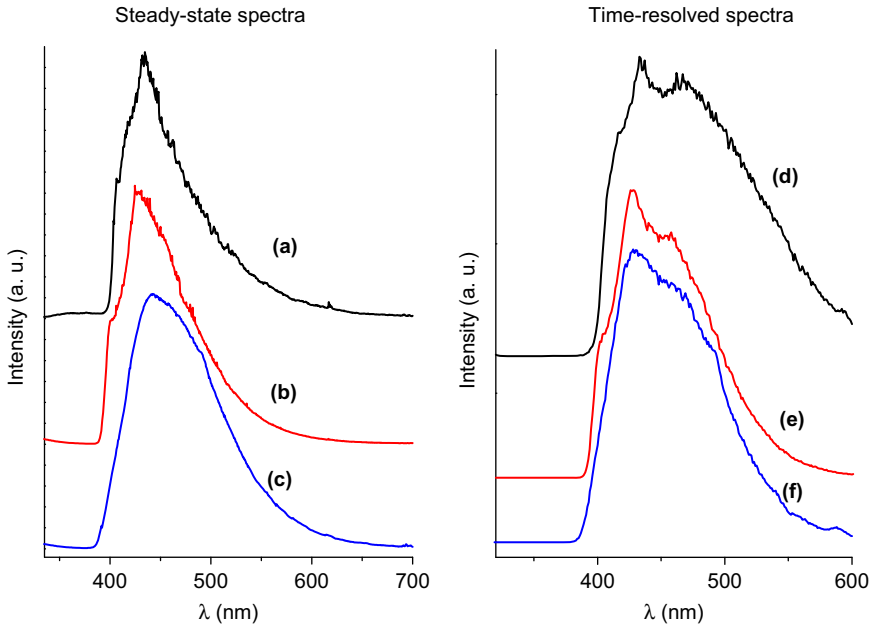

Fig. 3. Phosphorescence data of [Gd(EMA)$(H_2O)_2$], [Gd(TLA)$(H_2O)_4$] and [Gd(TMA)$(H_2O)_6$] complexes recorded at 77 K under excitation at 290 nm using the steady-state (a, b and c) and time-resolved (d, e and f) techniques.

Table 1
Lifetimes (τ) of the T state of BTC ligands and emitting ^5D_J states of Eu^{3+}(J=0) and Tb^{3+} (J=4) ions for the [RE(BTC)$(H_2O)_n$] complexes (n=2, 4 and 6), at 298 K.

Complex	Emitting state	τ (298 K)	x	y
Eu(EMA)$(H_2O)_2$]	$^5D_0$	0.379	0.67	0.31
[Eu(TLA)$(H_2O)_4$]	$^5D_0$	0.473	0.68	0.31
[Eu(TMA)$(H_2O)_6$]	$^5D_0$	0.230	0.68	0.31
[Gd(EMA)$(H_2O)_2$]	T_1	7.113	0.16	0.24
[Gd(TLA)$(H_2O)_4$]	T_1	2.210	0.15	0.16
[Gd(TMA)$(H_2O)_6$]	T_1	4.062	0.17	0.19
[Tb(EMA)$(H_2O)_2$]	$^5D_4$	1.135	0.33	0.56
[Tb(TLA)$(H_2O)_4$]	$^5D_4$	0.782	0.34	0.25
[Tb(TMA)]	$^5D_4$	1.572	0.37	0.54

Color coordinates (x, y) of the complexes are also presented.

luminescence sensitizations through intramolecular energy transfer from TLA and TMA ligands to Eu^{3+} ion are more efficient.

Emission spectra of the [Eu(BTC)$(H_2O)_n$] complexes (n=2, 4 and 6) in solid state recorded in the range from 370 to 800 nm, under excitation on BTC ligand bands at ~295 nm, at 77 K, show characteristic $^5D_0 \rightarrow {}^7F_J$ (J=0, 1, 2, 3 and 4) transitions of the Eu^{3+} ion, with the hypersensitive $^5D_0 \rightarrow {}^7F_2$ transition (at 617 nm) being the most prominent (Figs. 4d, e and f). The presence of the $^5D_0 \rightarrow {}^7F_2$ transition indicates that the Eu^{3+} ion is found in chemical environment without center of inversion, considering that Laporte's rule is slightly relaxed for 4f–4f transitions due to the mixing of opposite parity electronic configurations, produced by the odd components of a non-centrosymmetric ligand field. The emission spectra also present the f–f transitions: $^5D_1 \rightarrow {}^7F_0$ (526 nm), $^5D_1 \rightarrow {}^7F_1$ (536 nm), $^5D_1 \rightarrow {}^7F_2$ (552 nm) and $^5D_1 \rightarrow {}^7F_3$ (584 nm), but with very low intensities. The other feature optical data is that the emission spectra of all europium benzenetricarboxylate complexes do not exhibit the broad band of ligands (Fig. 4d, e and f), indicating an efficient intramolecular energy transfer from the BTC ligands to the Eu^{3+} ion, and these complexes act as light conversion molecular devices (LCMDs).

Fig. 4d shows the emission spectrum of the [Eu(TMA)$(H_2O)_6$] complex with (2J+1)-components for the $^5D_0 \rightarrow {}^7F_{0-4}$ transitions, suggesting the presence of only one site of symmetry around the europium ion. The local-ligand field splitting is also evident for $^5D_0 \rightarrow {}^7F_{0-4}$ transitions of the [Eu(TLA)$(H_2O)_4$] and [Eu(EMA)$(H_2O)_2$] complexes, however, presenting more than Stark (2J+1)-components, indicating that the Eu^{3+} ion occupies more than one site of symmetry (Figs. 4e and f). It is observed that, in general, emission spectra of complexes with TLA and EMA ligands present different profiles, reflecting changes in the chemical environment around the Eu^{3+} ion having different chemical environments with site symmetries of the type C_s, C_n or C_{nv}, which is expected to form the coordination polymers.

In order to get further information on the chemical environment of the Eu^{3+} ions for the [Eu(BTC)$(H_2O)_n$] complexes, experimental intensity parameters Ω_λ (λ=2 and 4), radiative rates (A_{0J}) for the $^5D_0 \rightarrow {}^7F_2$ and $^5D_0 \rightarrow {}^7F_4$ transitions and emission quantum efficiency (η) were determined (Table 2) according to Refs. [16,31].

$$A_{0\rightarrow J} = \frac{\sigma_{0\rightarrow 1} S_{0\rightarrow J}}{S_{0\rightarrow 1} \sigma_{0\rightarrow J}} A_{0\rightarrow 1} \quad (1)$$

where $\sigma_{0\rightarrow 1}$ and $\sigma_{0\rightarrow J}$ correspond to the energy barycenters of the $^5D_0 \rightarrow {}^7F_1$ and $^5D_0 \rightarrow {}^7F_J$ transitions (in cm^{-1}), respectively. In a similar way $S_{0\rightarrow 1}$ and $S_{0\rightarrow J}$ are the surface of the emission curve corresponding to the $^5D_0 \rightarrow {}^7F_1$ and $^5D_0 \rightarrow {}^7F_J$ transitions, respectively [32]. As it can be seen, for Eu^{3+} complexes the coefficients $A_{0\rightarrow J}$ are determined by taking the magnetic dipole $^5D_0 \rightarrow {}^7F_1$ transition as an internal standard since $A_{0\rightarrow 1}$ rate is almost insensitive to changes in the chemical environment around the europium ion with $A_{0\rightarrow 1} \cong 50\,s^{-1}$. The radiative contribution is estimated based only on the relative intensities of the $^5D_0 \rightarrow {}^7F_{0-4}$ transitions owing to the fact that the $^5D_0 \rightarrow {}^7F_{5,6}$ transitions are not observed experimentally [16].

The lifetimes (τ) of the [RE(BTC)$(H_2O)_n$] complexes (Table 1) were obtained from the luminescence decay curves using the equation $I(t)1 = I(0)\exp(-t/\tau)$ and a curve-fitting program. In the same system, the τ values of Tb^{3+} ion are higher than those of Eu^{3+} ion owing to the larger energy gap of terbium ion (14,800 cm^{-1}) compared with the europium gap (12,300 cm^{-1}).

It is possible to determine the emission quantum efficiency (η) of the $^5D_0$ emitting level of the Eu^{3+} ion, according to the

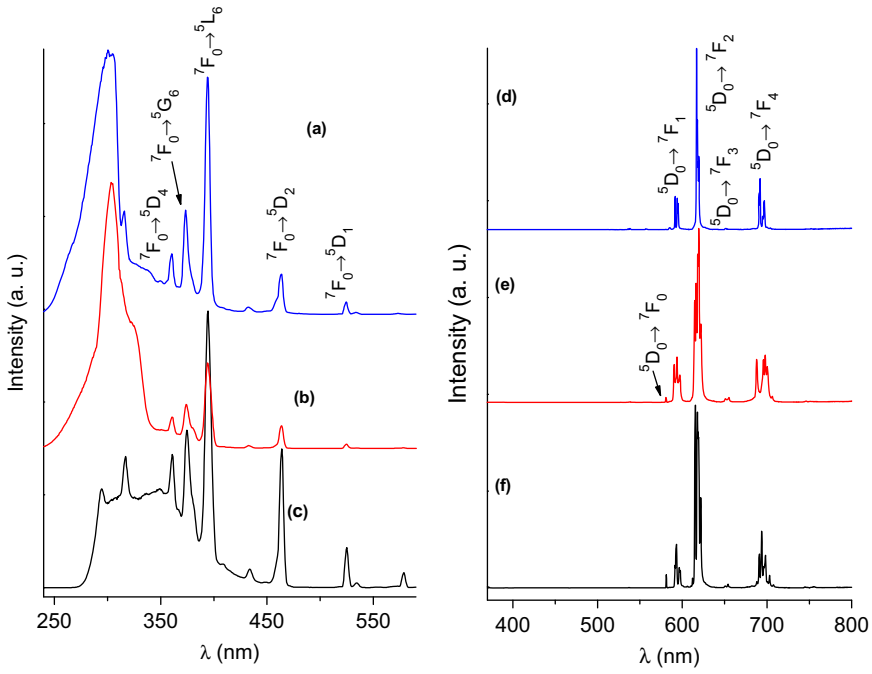

Fig. 4. Photoluminescence spectral data of the [Eu(BTC)$(H_2O)_n$] complexes (n=2, 4 and 6) in solid state recorded at 77 K. Excitation spectra obtained monitoring emission on the hypersensitive $^5D_0 \rightarrow {}^7F_2$ transition of the Eu^{3+} ion, at ~617 nm (a, b and c). Emission spectra recorded on BTC ligand bands at ~295 nm (d, e and f).

Table 2
Photoluminescent data of the [Eu(BTC)$(H_2O)_n$] complexes (n=2, 4 and 6) solid state.

Complex	Ω_2 10^{-20} cm^2	Ω_4 10^{-20} cm^2	A_{rad} (s^{-1})	A_{nrad} (s^{-1})	A_{tot} (s^{-1})	R_{02}	η (%)
[Eu(EMA)$(H_2O)_2$]	14.3	10.1	623	2015	2637	0.1200	24
[Eu(TLA)$(H_2O)_4$]	9.5	8.7	462	1653	2116	0.0279	22
[Eu(TMA)$(H_2O)_6$]	10.8	10.4	522	3820	4345	0.0003	12

The experimental intensity parameters (Ω_λ and R_{02}), radiative spontaneous emission coefficient A_{rad}, non-radiative spontaneous emission coefficient (A_{nrad}) and quantum efficiency (η) of the emitting $^5D_0$ level were obtained at room temperature (around 298 °C).

equation

$$\eta = \tau A_{rad} \tag{2}$$

where the total decay rate,

$$A_{tot} = \frac{1}{\tau} = A_{rad} + A_{nrad},$$

where $A_{rad}(=\sum A_{0\rightarrow J})$ and A_{nrad} are the radiative and non-radiative rates, respectively. Thus, based on the experimental lifetime (τ) of the $^5D_0$ emitting level and A_{rad} rate, it was possible to determine the non-radiative rates (A_{nrad}). The experimental values of the radiative (A_{rad}) and non-radiative (A_{nrad}) rates, and emission quantum efficiency (η) are presented in Table 2. The emission quantum efficiency data show that the higher values of η, 22% for [Eu(TLA)$(H_2O)_4$] and 24% for [Eu(EMA)$(H_2O)_2$] complexes, are due to the lower number of water molecules in the complexes, where this fact is reflected by the lower contribution of non-radiative (A_{nrad}) arising from the OH oscillator of water molecules. On the other hand, the six water molecules in the [Eu(TMA)$(H_2O)_6$] complex contribute to the higher luminescence quenching and consequently lower value of η (12%).

From the emission spectra of Eu^{3+} complexes, the experimental intensity parameters (Ω_λ, λ=2 and 4) may be estimated using the $^5D_0 \rightarrow {}^7F_2$ and $^5D_0 \rightarrow {}^7F_4$ transitions, respectively, and expressing the emission intensity in terms of the area under the emission curve. The Ω_6 intensity parameter is not included in this study since the $^5D_0 \rightarrow {}^7F_6$ transition is usually not observed for these complexes. The coefficient of spontaneous emission, A, is given by equation

$$A = \frac{4e^2\omega^3}{3hc}\chi\sum_\lambda \Omega_\lambda \langle {}^7F_J||U^{(\lambda)}||{}^5D_0\rangle^2 \tag{3}$$

where $\chi = n(n+2)^2/9$ is the Lorentz local field correction and n is the index of refraction of the medium. An average index of refraction equal to 1.5 has been used for these complexes. The quantities $\langle {}^7F_J||U^{(\lambda)}||{}^5D_J\rangle^2$ are the square reduced matrix elements and are equal to 0.0032 and 0.0023 for J=2 and 4, respectively [33]. Since the intensity of the magnetic dipole transition $^5D_0 \rightarrow {}^7F_1$ is relatively insensitive to the chemical environment of the Eu^{3+} ion, it may be used as the internal standard (reference transition) to avoid the difficulties in the experimental measurement of absolute emission intensities [34,35].

Analysis of the experimental intensity parameters (Ω_2 and Ω_4) gives a general trend concerning the link between the numbers H_2O and BTC ligands in the first coordination sphere of Eu^{3+} ion. As a matter of fact, the oxygen atoms that belong to EMA, TLA and TMA ligands differ from their polarizabilities.

Values of experimental intensity parameters Ω_λ (λ=2 and 4) for the $^5D_0 \rightarrow {}^7F_2$ and $^5D_0 \rightarrow {}^7F_4$ transitions for Eu^{3+}-(BTC) complexes are presented in Table 2. The high values of the intensity Ω_2 parameter ($\gg 1\times10^{-20}$ cm^2) might be interpreted as a consequence of two concurrent factors. The first one is the very low symmetry around the Eu^{3+} ion, allowing the appearance of all odd-rank components in the sums-over-ligands. The second factor

is related to the hypersensitive behavior of the $^5D_0 \rightarrow {}^7F_2$ transition [16], suggesting that the dynamic coupling mechanism is operative and that the chemical environment around the metal ion is highly polarizable, possibly due to the strong delocalization of the carboxylate oxygen charge.

The delocalization of the π-electrons of the chelate rings in EMA, TLA and TMA ligands increases the polarizability of the oxygen atoms in the $[Eu(BTC)(H_2O)_4]$ complexes with less number of H_2O molecules. Consequently, when four or six water molecules are coordinated to the metal ion, the chemical environment around the europium ion becomes less polarizable compared to those with only two H_2O molecules, which is reflected on the highest value of $\Omega_2 = 14.3 \times 10^{-20}\,cm^2$ (Table 2).

Table 2 presents also the R_{02} intensity parameter, which is the ratio between the intensities of the $^5D_0 \rightarrow {}^7F_0$ and $^5D_0 \rightarrow {}^7F_2$ transitions. The R_{02} parameter may give information on the *J*-mixing effect associated with the $^5D_0 \rightarrow {}^7F_0$ transition as described in detail in Ref. [36]. In this case, this effect is mainly due to the mixing between the $^7F_2$ manifold and the $^7F_0$ level though the rank-two components of the ligand field. By comparison between the three Eu^{3+}-(BTC) complexes the following order for the magnitude of the *J*-mixing effect is proposed: EMA $>$ TLA $\gg$ TMA.

3.2.3. *Luminescence of Tb^{3+}-BTC complexes*

The $[Tb(BTC)_3(H_2O)_n]$ complexes exhibit a highly intense green emission color under UV excitation. Fig. 5a–c shows the excitation spectra of the Tb^{3+} complexes recorded in the spectral range from 240 to 550 nm, at low temperature (77 K), with emission monitored on the $^5D_4 \rightarrow {}^7F_5$ transition at 545 nm. The spectral data consist of broad bands of high absorption intensities in the spectral range from 240 to 370 nm, with maximum at 295 nm, which is attributed to the $S_0 \rightarrow S_1$ transitions of the EMA, TLA and TMA ligands. In addition to these bands, narrow bands arising from 4f–4f intraconfigurational transitions from the ground-state $^7F_6$ level to the $^5L_8$ (339 nm), $^5L_9$ (351 nm), $^5G_5$ (358 nm), $^5L_{10}$ (368 nm), $^5G_6$ (377 nm) and $^5D_4$ (486 nm) excited levels are also observed. However, the relative intensity of the broad band is higher than the 4f–4f transitions centered on the Tb^{3+} ion. It is also observed that the indirect excitation processes of the metal ion, via chromophore groups from the ligands, are more operative than in $^7F_6 \rightarrow {}^5L_J$ transitions for the Tb^{3+}-BTC complexes.

The emission spectra of Tb^{3+}-(BTC) complexes, in the solid state, were registered in the range 320–700 nm under excitation at ligand transitions (300 nm) at liquid nitrogen temperature, as shown in Fig. 5d–f. The luminescence spectra of Tb^{3+}-complexes ($4f^8$ configuration) generally exhibit characteristic narrow emission bands arising from the $^5D_4 \rightarrow {}^7F_J$ transitions (J=0–6) of trivalent terbium ion, which are assigned as follows: $^5D_4 \rightarrow {}^7F_0$ (682 nm), $^5D_4 \rightarrow {}^7F_1$ (669 nm), $^5D_4 \rightarrow {}^7F_2$ (653 nm), $^5D_4 \rightarrow {}^7F_3$ (621 nm), $^5D_4 \rightarrow {}^7F_4$ (587 nm), $^5D_4 \rightarrow {}^7F_5$ (545 nm) and $^5D_4 \rightarrow {}^7F_6$ (490 nm) with the $^5D_4 \rightarrow {}^7F_5$ transition as the most prominent band of the Tb^{3+} ion. The emission spectral data do not exhibit a broad band from the triplet state of the EMA, TLA and TMA ligands in the spectral range 370–550 nm, indicating an efficient energy transfer from the T state of the ligand to the emitting $^5D_4$ level of the terbium ion.

The large gaps between the emitting $^5D_4$ levels and final ^7F_J levels of Tb^{3+} compounds are around 15,000 cm^{-1}. They usually exhibit a green color in the presence of UV radiation [37]. In contrast to the Eu^{3+} ion, detailed analyses of energy-level structure and symmetry site around the Tb^{3+} ion are not possible, since the $^5D_4$ emitting level and $^7F_6$ Stark level are nine-fold and thirteen-fold degenerated, respectively [38]. The $^5D_4 \rightarrow {}^7F_5$ transition is the best luminescence probe for the terbium ion [39]. Otherwise, the sensitization pathway in luminescent Tb^{3+} complexes is similar to those of Eu^{3+} complexes. However, the triplet states of the β-diketonate (acetylacetonate-acac) [16] and carboxylate [39] ligands have to be located above or in resonance with the excited $^5D_4$ level ($\sim$20,400 cm^{-1}). The same behavior was observed for the Tb^{3+}-(BTC) complexes (BTC=TMA, TLA and EMA).

According to Reinhoudt's empirical rule [40] the intersystem crossing process will be effective when the energy gap between S

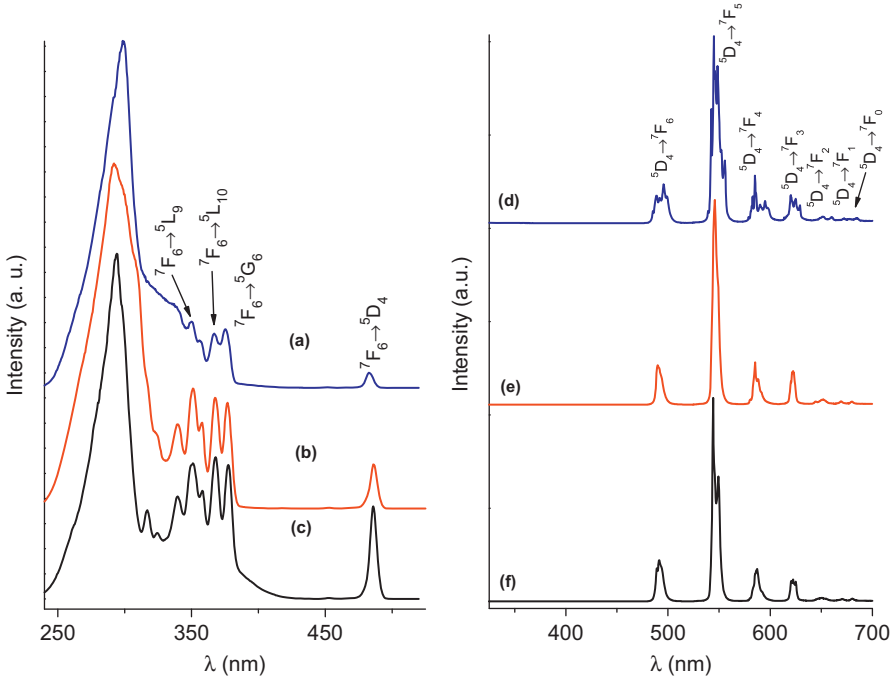

Fig. 5. Photoluminescence spectral data of the [Tb(TMA)] and $[Tb(BTC)(H_2O)_n]$ complexes (BTC=TMA, TLA and EMA; n=2, 4 and 6) in solid state recorded at 77 K. Excitation spectra obtained monitoring emission on the $^5D_4 \rightarrow {}^7F_5$ transition of the Tb^{3+} ion at $\sim$545 nm (a, b and c). Emission spectra recorded on the BTC ligand bands at $\sim$295 nm (d, e and f).

and T excited states of the ligands, $\Delta E[S(^1\pi\pi)\text{-}T(^3\pi\pi)]$, is around 5000 cm^{-1}. As the intersystem crossing process of the BTC ligands are efficient, it can be assumed that the singlet state present energy at 30,000 cm^{-1} for these carboxylate groups. In addition, Latva et al. [41] reported that the best intramolecular energy transfer from a T ligand to emitting $^5D_4$ level of Tb^{3+} ion occurs when the energy gap between the T state of the ligand and the first emitting $^5D_4$ level of the Tb^{3+} is higher than 2000 cm^1. For these complexes, the energy gaps are in the range of 4600–5200 cm^1 that avoids the possibility of an energy back-transfer from the metal ion [42]. The photoluminescent data suggest that the BTC ligands act as efficient *antennas* sensitizing the luminescence of the Tb^{3+} ion for these complexes.

Fig. 6 shows the photographs of the $[RE(TLA)(H_2O)_4]$ complexes (where RE^{3+}=Eu^{3+}, Gd^{3+} and Tb^{3+}) taken at room temperature (~298 K), which exhibit red, blue and green emissions colors. These primary colors arise mainly from the narrow bands of $^5D_0 \rightarrow {}^7F_2$ and $^5D_4 \rightarrow {}^7F_5$ transitions of the Eu^{3+} and Tb^{3+} ions, respectively. On the other hand, the blue emission color of the Gd^{3+}-complex is owing to the broad band of T→S transition from the BTC ligand phosphorescence band. Fig. 6 also shows the partial energy-level diagram of Eu^{3+}, Gd^{3+} and Tb^{3+} ions containing their excited and ground states.

The Eu^{3+}-BTC-complexes present similar (*x*,*y*) color coordinates (Table 1) in the red region of the CIE chromaticity diagram (*Commission Internationale de l'Eclairage*) from narrow 4f–4f transitions of rare earth ions (Fig. 7) [43]. The anhydrous [Tb(TMA)] complex displays the green yellow emission color when compared with $[Tb(EMA)(H_2O)_2]$ and $[Tb(TLA)(H_2O)_4]$ complexes that show green color. In case of Gd^{3+}-BTC-complexes blue emission colors were observed, arising from the broad band ligand centered transitions of BTC^{3-} anion. As it can be seen, these complexes present emissions containing the three primary colors

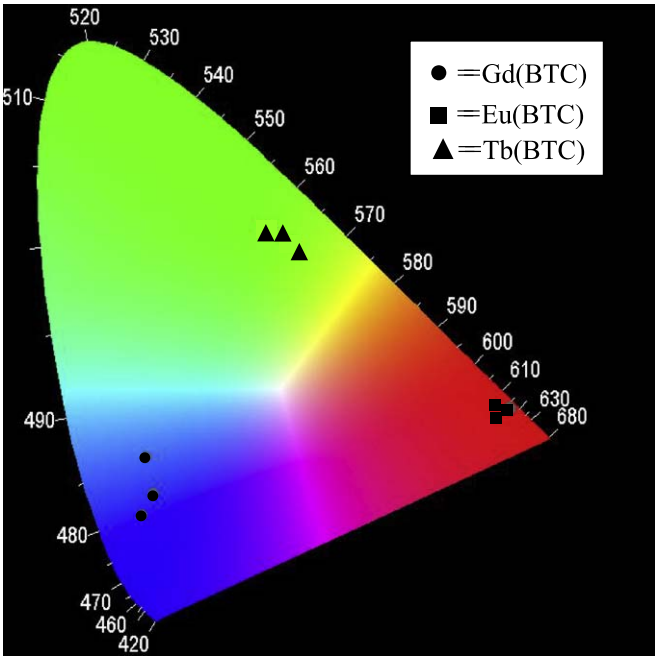

Fig. 7. Chromaticity coordinates from emission spectra of the $[RE(BTC)(H_2O)_n]$ complexes (RE^{3+}=Eu, Gd and Tb; BTC=EMA, TLA and TMA; *n*=2, 4 and 6).

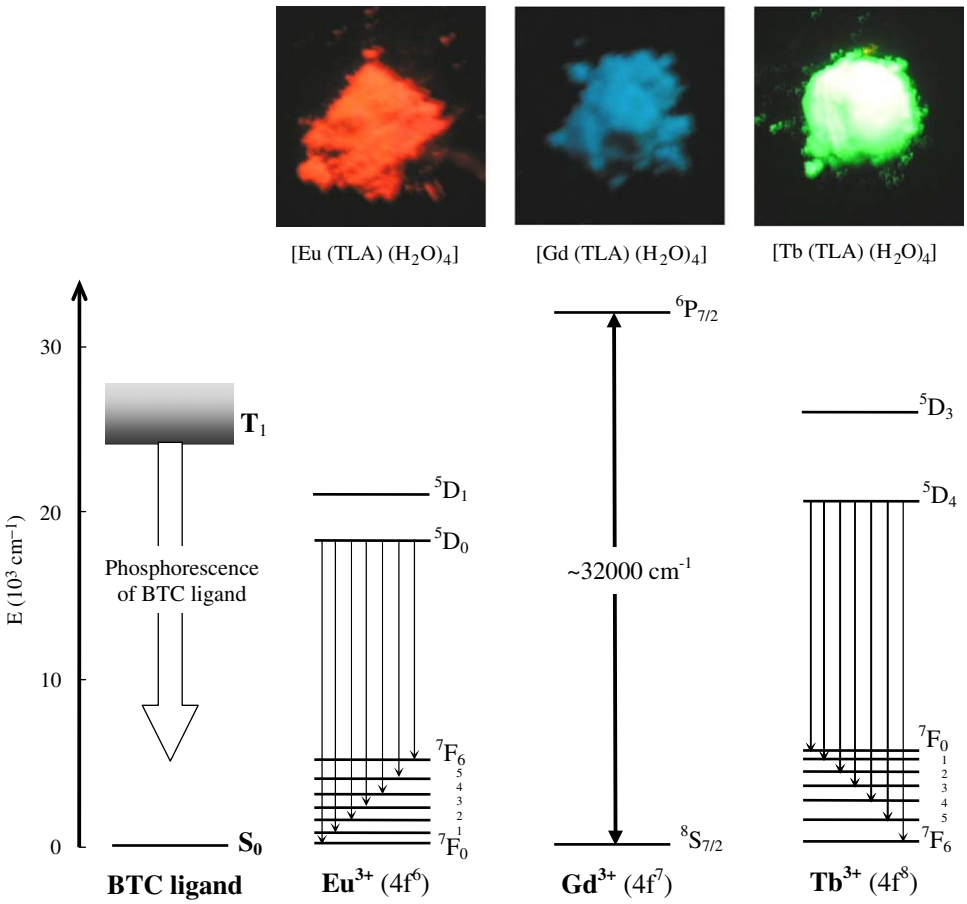

Fig. 6. Partial energy-level diagram of rare earth ions (Eu^{3+}, Gd^{3+} and Tb^{3+}). Triplet states of BTC ligands are shown on the left and arrows indicate emitting levels (photographs were obtained after UV irradiation).

(red, green and blue) that can be applied in tricolor devices. The Eu^{3+} and Tb^{3+} complexes act as light conversion molecular devices (LCMDs) and produce monochromatic emission colors.

4. Conclusion

In this work emitting Eu^{3+}, Gd^{3+} and Tb^{3+} complexes were prepared, containing the benzenetricarboxylate ligands (BTC) that exhibit red, blue and green emission colors, respectively. Phosphorescence data of Gd^{3+}-(BTC) complexes showed highly intensity blue emission at room temperature. The triplet states of the BTC^{3-} anions have energy higher than the main emitting states of Eu^{3+} ($^5D_0$) and Tb^{3+} ($^5D_4$), indicating that BTC ligands act as intramolecular energy donors for these metal ions. The high values of experimental intensity parameters (Ω_2) of Eu^{3+}-(BTC) complexes indicate that the europium ion is in a highly polarizable chemical environment. The emission quantum efficiency of the emitting $^5D_0$ level data shows that the highest value of η (24%) for the $[Eu(EMA)(H_2O)_2]$ complex is due to the lower number of coordinated water molecules arising from the lower contribution of non-radiative (A_{nrad}) from the OH oscillator. The Tb^{3+}-(BTC) complexes exhibit sharp green emission intensities assigned to the characteristic $^5D_4 \rightarrow {}^7F_J$ (J=0–6) transitions, indicating that the BTC ligands are good sensitizers. Photoluminescence data showed that the Eu^{3+}, Gd^{3+} and Tb^{3+} complexes act as efficient light conversion molecular devices (LCMDs) and can be used as red, green and blue emitter luminescent materials.

Acknowledgements

The authors thank Conselho Nacional de Desenvolvimento Científico e Tecnológico (CNPq), Fundação de Amparo à Pesquisa do Estado de São Paulo (FAPESP), Rede de Nanotecnologia Molecular e de Interfaces (RENAMI) and Instituto do Milênio de Materiais Complexos (IM^2C) for financial support.

References

[1] Y.W. Li, R.T. Yang, AIChE J 54 (2008) 269.
[2] U. Mueller, M. Schubert, F. Teich, H. Puetter, K. Schierle-Arndt, J. Pastre, J. Mater. Chem. 16 (2006) 626.
[3] D.J. Collins, H.C. Zhou, J. Mater. Chem. 30 (2007) 3154.
[4] U. Ravon, M.E. Domine, C. Gaudillere, A. Desmartin-Chomel, D. Farrusseng, New J. Chem. 32 (2008) 937.
[5] G. Ferey, Chem. Soc. Rev. 37 (2008) 191.
[6] B. Chen, Y. Yang, F. Zapata, G. Lin, G. Qian, E.B. Lobkovsky, Adv. Mater. 19 (2007) 1693.
[7] Z. Rzaczynska, A. Ostasz, S. Pikus, J. Therm. Anal. Calorim. 82 (2005) 347.
[8] R. Lyszczek, J. Therm. Anal. Calorim. 90 (2007) 533.
[9] R. Lyszczek, J. Therm. Anal. Calorim. 91 (2008) 595.
[10] M.A. Braverman, R.M. Supkowski, R.L. LaDuca, J. Solid State Chem. 180 (2007) 1852.
[11] N. Hao, F. Liu, E. Wang, R. Huang, Y. Li, C. Hu, Inorg. Chem. Commun. 6 (2003) 728.
[12] Z. Li, G. Zhu, X. Guo, X. Zhao, Z. Jin, S. Qiu, Inorg. Chem. 46 (2007) 5174.
[13] N.L. Rosi, J. Kim, M. Eddaoudi, B. Chen, M. O'Keeffe, O.M. Yaghi, J. Am. Chem. Soc. 127 (2005) 1504.
[14] J. Yang, Q. Yue, G.-D. Li, J.-J. Cao, G.-H. Li, J.-S. Chen, Inorg. Chem. 45 (2006) 2857.
[15] S. Surble, C. Serre, F. Millange, F. Pelle, G. Ferey, Solid State Sci. 7 (2005) 1074.
[16] H.F. Brito, O.L. Malta, M.C.F.C. Felinto, E.E.S. Teotonio, Luminescence phenomena involving metal enolates, in: J. Zabicky, (Ed.), Patai Series: the Chemistry of Metal Enolates, John Wiley & Sons Ltd. (chapter 3), 2009, pp. 131–184.
[17] N. Sabbatini, M. Guardigli, J.M. Lehn, Coord. Chem. Rev. 123 (1993) 201.
[18] J.-C.G. Bünzli, C. Piguet, Chem. Soc. Rev. 34 (2005) 1048.
[19] R.C. Evans, P. Douglas, C.J. Winscom, Coord. Chem. Rev. 250 (2006) 2093.
[20] J. Kai, D.F. Parra, H.F. Brito, J. Mater. Chem. 18 (2008) 4549.
[21] G.E. Buono-Core, H. Li, B. Marciniak, Coord. Chem. Rev. 99 (1990) 55.
[22] J. Kido, Y. Okamoto, Chem. Rev. 102 (2002) 2357.
[23] R. Reyes, M. Cremona, E.E.S. Teotonio, H.F. Brito, O.L. Malta, Thin Solid Films 469 (2004) 59.
[24] B. Chen, L. Wang, F. Zapata, G. Qian, E.B. Lobkovsky, J. Am. Chem. Soc. 130 (2008) 6718.
[25] M.P. Bemquerer, C. Bloch, H.F. Brito, E.E.S. Teotonio, M.T.M. Miranda, J. Inorg. Biochem. 91 (2002) 363.
[26] K. Nakamoto, Infrared and Raman Spectra of Inorganic and Coordination Compounds, fifth ed., Wiley, New York, 1997.
[27] G.B. Deacon, R. Phillips, J. Coord. Chem. Rev. 33 (1980) 227.
[28] H.F. Brito, G.K. Liu, J. Chem. Phys. 112 (2000) 4334.
[29] S. Tobita, M. Arakawa, I. Tanaka, J. Phys. Chem. 88 (1985) 2697.
[30] E.E.S. Teotonio, M.C.F.C. Felinto, H.F. Brito, O.L. Malta, A.C. Trindade, R. Najjar, W. Strek, Inorg. Chim. Acta 357 (2004) 451.
[31] G.F. de Sá, O.L. Malta, C.D. Donega, A.M. Simas, R.L. Longo, P.A. Santa-Cruz, E.F. Silva, Coord. Chem. Rev. 196 (2000) 165.
[32] E.E.S. Teotonio, G.M. Fett, H.F. Brito, W.M. Faustino, G.F. de Sa, M.C.F.C. Felinto, R.H.A. Santos, J. Lumin. 128 (2008) 190.
[33] W.T. Carnall, H. Crosswhite, H.M. Crosswhite, Energy Level Structure and Transition Probabilities of the Trivalent Lanthanide in LaF_3, Argonne National Laboratory, Argonne, Ilinois, 1977 4493.
[34] L.D. Carlos, Y. Messaddeq, H.F. Brito, R.A.S. Ferreira, V. de Zea Bermudez, S.J.L. Ribeiro, Adv. Mater. 12 (2000) 594.
[35] D.B. Ambili Raj, S. Biju, M.L. P Reddy, Inorg. Chem. 47 (2008) 8091.
[36] O.L. Malta, W.M. de Azevedo, E.G. de Araújo, G.F. de Sá, J. Lumin. 26 (1982) 337.
[37] F.S. Richardson, Chem. Rev. 82 (1982) 541.
[38] D.F. Parra, A. Mucciolo, H.F. Brito, J. Appl. Polym. Sci. 94 (2004) 865.
[39] E.E.S. Teotonio, G.M. Fett, H.F. Brito, A.C. Trindade, M.C.F.C. Felinto, Inorg. Chem. Commun. 10 (2007) 867.
[40] F.J. Steemers, W. Verboon, D.N. Reinhoudt, E.B. Vander Tol, J.W. Verhoeven, J. Am. Chem. Soc. 117 (1995) 9408.
[41] M. Latva, H. Takalo, V.-M. Mukkala, C. Matachescuc, J.C. Rodriguez Ubisd, J. Kankare, J. Lumin. 75 (1997) 149.
[42] S. Biju, M.L.P. Reddy, R.O. Freire, Inorg. Chem. Commun. 10 (2007) 393.
[43] P.A. Santa-Cruz, F.S. Teles, Spectra Lux Software v.2.0 Beta, Ponto Quântico Nanodispositivos, RENAMI, 2003.